

Article

Determination of Activation Energy from Decolorization Reactions of Synthetic Dyes by Fenton Processes Using the Behnajady–Modirshahla–Ghanbary Kinetic Model

Márcio Daniel Nicodemos Ramos , Juan Pablo Pereira Lima  and André Aguiar * 

Institute of Natural Resources, Federal University of Itajubá, Itajubá 37500-903, MG, Brazil; marcio_daniel_ramos@hotmail.com (M.D.N.R.); juanpablotp3@hotmail.com (J.P.P.L.)

* Correspondence: aguiar@unifei.edu.br; Tel.: +55-35-36291803

Abstract: The present work used the Behnajady–Modirshahla–Ghanbary (BMG) kinetic model to determine the initial reaction rates ($1/m$), which were used to calculate the activation energy (E_a) from the decolorization of synthetic dyes by Fenton processes ($\text{Fe}^{2+}/\text{H}_2\text{O}_2$, $\text{Fe}^{2+}/\text{H}_2\text{O}_2/\text{reducer}$ and $\text{Fe}^{3+}/\text{H}_2\text{O}_2/\text{reducer}$). When increasing the temperature and adding Fe^{3+} -reducing compounds (3-Hydroxyanthranilic Acid, Hydroquinone, Gallic Acid, Cysteine or Ascorbic Acid), increases in the $1/m$ values were observed. When studying the classical Fenton reaction ($\text{Fe}^{2+}/\text{H}_2\text{O}_2$), almost all added reducers had decreased E_a . For example, 3-Hydroxyanthranilic Acid decreased the E_a related to the decolorization of the Phenol Red dye by 39%, while Ascorbic Acid decreased the E_a of Safranin T decolorization by 23%. These results demonstrate that the reducers increased the initial reaction rate and decreased the energy barrier to improve Fenton-based decolorization of dyes. When comparing the reaction systems in presence of reducers ($\text{Fe}^{n+}/\text{H}_2\text{O}_2/\text{reducer}$), the reactions initially containing Fe^{2+} presented lower E_a than reactions catalyzed by Fe^{3+} . That way, the activation energy obtained through the $1/m$ values of the BMG model highlighted the pro-oxidant effect of reducers in Fenton processes to degrade dyes.



Citation: Ramos, M.D.N.; Lima, J.P.P.; Aguiar, A. Determination of Activation Energy from Decolorization Reactions of Synthetic Dyes by Fenton

Processes Using the Behnajady–Modirshahla–Ghanbary Kinetic Model. *Catalysts* **2024**, *14*, 273. <https://doi.org/10.3390/catal14040273>

Academic Editors: Vincenzo Vaiano and Enric Brillas

Received: 29 January 2024

Revised: 26 March 2024

Accepted: 16 April 2024

Published: 18 April 2024

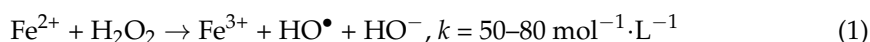


Copyright: © 2024 by the authors. Licensee MDPI, Basel, Switzerland. This article is an open access article distributed under the terms and conditions of the Creative Commons Attribution (CC BY) license (<https://creativecommons.org/licenses/by/4.0/>).

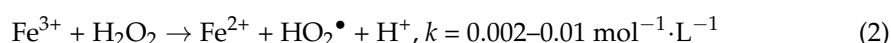
Keywords: Fenton reaction; reducer; hydroxyl radical; kinetics; advanced oxidative process

1. Introduction

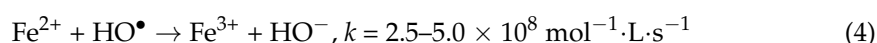
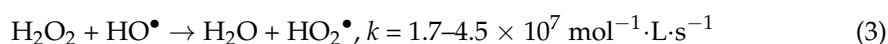
Several technologies have been evaluated to treat effluents from the textile industry, and processes based on the Fenton reaction have been standing out in removing more pollutants [1]. Conventional processes to treat these effluents do not properly remove or degrade the more complex structures of the dyes [2,3]. Furthermore, pollutants are generally transferred from the liquid phase to the form of sludge, which also needs to be treated and disposed of appropriately [4,5]. Advanced oxidation processes based on the Fenton reaction have demonstrated great efficiency in the degradation and mineralization of different classes of dyes [6–9]. The Fenton reaction is based on the catalytic degradation of hydrogen peroxide by ferrous ions (Reaction (1)) to generate hydroxyl radical (HO^\bullet). This free radical has a high standard reduction potential ($E^\circ = 2.8 \text{ V}$), and can degrade several recalcitrant pollutants, including dyes.



By adding Fe^{3+} ions at the beginning, instead of Fe^{2+} , there is the Fenton-like reaction (Reaction (2)). However, the radical formed is hydroperoxyl (HO_2^\bullet), which has a lower standard reduction potential ($E^\circ = 1.42 \text{ V}$) and, consequently, less effectiveness when compared to HO^\bullet . Despite being very slow, the second reaction is important as it regenerates Fe^{2+} from Fe^{3+} , allowing it to participate again in the first reaction [10–12].



A limitation of processes based on the classical Fenton reaction is the low rate of reduction of Fe^{3+} by Reaction (2) compared to the oxidation of Fe^{2+} through Reaction (1). This promotes the accumulation of ferric ions that tend to precipitate as hydr(oxides), making the catalyst unavailable. An alternative to increasing the production of hydroxyl radicals in the reaction medium is to increase the concentrations of the reactants. However, when increasing the catalyst concentration, there is an increase in the formation of iron-containing sludge, while an excess of H_2O_2 or catalyst would reduce the degradation efficiency, as the HO^\bullet also reacts with the H_2O_2 (Reaction (3)) and Fe^{2+} (Reaction (4)), instead of reacting only with target pollutants [12,13].



Certain organic compounds can minimize unwanted accumulation of Fe^{3+} due to the constant regeneration of Fe^{2+} (which is faster compared to H_2O_2), therefore enabling greater production of HO^\bullet radicals in the treatments [10]. Several reducing compounds have been tested, many of which are phenolic. When reducing Fe^{3+} to Fe^{2+} , phenolic reducers are converted to a semiquinone radical, which can also reduce Fe^{3+} and convert into its respective quinone. The latter can be regenerated to the semiquinone radical or even be oxidized by Fe^{3+} into smaller molecules, including CO_2 [14,15]. Therefore, the degradation and mineralization of the phenolic reducer and its intermediates may be desirable to minimize secondary pollution problems. The amino acid Cysteine and Ascorbic Acid present behavior very similar to phenols, considering the regeneration of Fe^{2+} in Fenton processes [16–19]. Figure 1 presents some reactions involving Fenton reagents and a reducing compound to degrade a target dye.

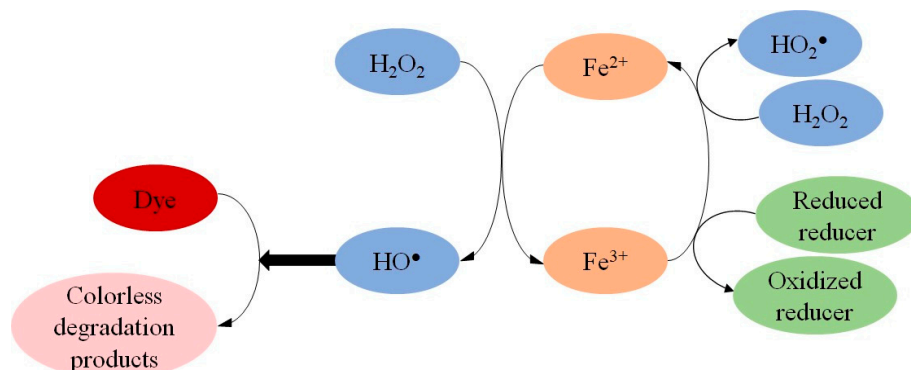


Figure 1. Reactions involved between Fe ions, H_2O_2 , reducer, and a dye.

An appropriate way to evaluate the effect of a reducing compound on Fenton processes is to evaluate the reaction kinetics of experimental data. In several studies by our research group, it was found that the first-order reaction model has been the one that best fits data on dye decolorization reactions by Fenton/reducer processes [20–23]. In turn, the second-order kinetic model was the one that best adjusted the results of the decolorization of two dyes [21,24]. Another kinetic model that was used in these studies and that fitted well much of the experimental data was that first used by Chan and Chu [25], being more commonly known as Behnajady–Modirshahla–Ghanbary (BMG). It was developed as a way to evaluate the degradation of pollutants by classical Fenton reaction, which were not described by conventional reaction kinetics models [26].

The BMG model is expressed by Equation (5), and is shown in its linearized form by Equation (6).

$$\frac{C_t}{C_0} = 1 - \left[\frac{t}{(m + b \cdot t)} \right] \quad (5)$$

$$\frac{t}{\left[1 - \left(\frac{C_t}{C_0}\right)\right]} = m + b \cdot t \quad (6)$$

where C_0 and C_t are the dye concentration values at the initial time and at a certain time t , respectively, while m (intercept) and b (slope) are the two intrinsic constants of the model. To interpret them, Equation (6) must be derived, as shown in Equation (7).

$$\frac{dC/C_0}{dt} = \frac{-m}{(m + b \cdot t)^2} \quad (7)$$

When time t is small or close to zero, the slope obtained can be solved according to Equation (8). Therefore, the greater $1/m$, the greater the initial rate of degradation of the target pollutant. On the other hand, when the time is long and approaches infinity, it is possible to obtain the maximum theoretical oxidation capacity ($1/b$), according to Equation (9). This shows that the maximum value of $1/b$ is 1 when the final concentration is null.

$$\frac{dC/C_0}{dt} = -\frac{1}{m} \quad (8)$$

$$\frac{1}{b} = 1 - \frac{C_{t \rightarrow \infty}}{C_0} \quad (9)$$

Such mathematical observations can be better observed in Figure 2 with the extreme values of time ($t = 0$ and $t = \infty$).

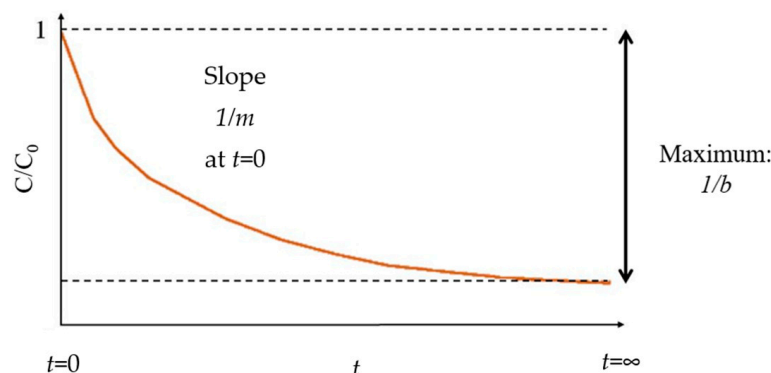


Figure 2. A linear way of representing the BMG model. This figure was reproduced from Behnadjy et al. [26], with permission from Elsevier (license number 5735830415425).

The decolorization of some dyes by $\text{Fe}^{2+}/\text{H}_2\text{O}_2$ has been well described by the BMG model, particularly due to the two-stage reaction behavior: one first and faster, followed by another that is slower. The first stage has been attributed to the reaction between Fe^{2+} and H_2O_2 , resulting in HO^\bullet radicals, and the second stage refers to the accumulation of Fe^{3+} (or low regeneration of Fe^{2+}) that reacts with H_2O_2 to form weaker radicals (such as HO_2^\bullet) [8,26–31]. On the other hand, when using Fe^{3+} as a catalyst at the beginning of reactions, decolorization does not usually have two stages, and the BMG model has been somewhat less adequate to describe them. When evaluating heterogeneous Fenton-like reaction, using natural schorl as catalyst, Xu et al. [32] also found that the BMG model did not fit the Methyl Orange decolorization data. From this perspective, previous studies by our research group corroborated these behaviors, as the BMG model fitted well to the decolorization reactions with Fe^{2+} , while those with Fe^{3+} were not well described by this model. Interestingly, when Ascorbic Acid, Gallic Acid, 3-Hydroxyanthranilic Acid or Hydroquinone was added to the system $\text{Fe}^{3+}/\text{H}_2\text{O}_2$, the BMG model adjusted well to the experimental data, indicating that these compounds reduced Fe^{3+} to Fe^{2+} rapidly, causing the decolorization to present two phases [20,21,23,24].

Assessing the activation energy (E_a) of reactions involved in Fenton processes is an important way of analyzing the pro-oxidant effect of reducers. To do this, it is necessary to carry out the reaction at different temperatures, calculate the rate constants, and then obtain E_a [33]. In previous works by our research group, when E_a was calculated, the reaction rate constants obtained through classical kinetic models were generally used and best fit the majority of experimental data, being of first-order [20–23] or second-order [21,24]. As the BMG model also fitted well with much of the experimental data in these studies, the $1/m$ values could also be used to calculate E_a . When evaluating the degradation of an herbicide by $\text{Fe}^{2+}/\text{H}_2\text{O}_2$ at different temperatures, Santos et al. [34] used this kinetic model to interpret their results. The values of $1/m$ obtained replaced the reaction rate constant (k) in the Arrhenius equation, allowing them to find an E_a of $49.3 \text{ kJ}\cdot\text{mol}^{-1}$. To the best of our knowledge, no studies have been conducted to calculate the E_a using $1/m$ values from the Fenton-based degradation of different dyes used as target pollutants.

Therefore, the present study aimed to continue studies of reaction kinetics based on the degradation of synthetic dyes via Fenton processes mediated by Fe^{3+} -reducing compounds. As a novelty, this work evaluated the activation energy (E_a) from the decolorization of various dyes by Fenton processes ($\text{Fe}^{2+}/\text{H}_2\text{O}_2$, $\text{Fe}^{2+}/\text{H}_2\text{O}_2/\text{reducer}$ and $\text{Fe}^{3+}/\text{H}_2\text{O}_2/\text{reducer}$) using the values of $1/m$ from the BMG reaction kinetics model [34]. For this purpose, the values of $1/m$ obtained from previous studies developed by our research group [20–24] were used in the present work. In addition, comparisons were made between E_a values calculated using $1/m$ and those obtained from the rate constants (k_1 , k_2) of conventional kinetic models.

2. Results and Discussion

2.1. Data for $1/m$ from Decolorization Reactions of Different Dyes Using Fenton Processes

Figure 3 shows the $1/m$ values obtained from previous studies by our research group. Only data referring to reactions that were well described by the BMG model ($R^2 > 0.9$) were used here; that is, all data related to the $\text{Fe}^{2+}/\text{H}_2\text{O}_2$ and $\text{Fe}^{2+}/\text{H}_2\text{O}_2/\text{reducer}$ systems, in addition to specific ones from $\text{Fe}^{3+}/\text{H}_2\text{O}_2/\text{reducer}$ in presence of 3-Hydroxyanthranilic Acid, Hydroquinone, Gallic Acid or Ascorbic Acid. In general, it was found that the $1/m$ values increased as a function of temperature, regardless of the target dye and the reaction system. This aspect can be explained by the increase in the number of collisions between reactant molecules with increasing temperature, promoting greater formation of free radicals [35,36]. For example, the value of $1/m$ referring to the $\text{Fe}^{2+}/\text{H}_2\text{O}_2/3\text{-Hydroxyanthranilic Acid}$ system was 10 times higher at 50°C than at 20°C . The increase in the value of $1/m$ as a function of temperature has also been observed in other studies that evaluated the Fenton-based degradation of dyes [27,37], including Methyl Orange [32].

Furthermore, it was noted that the temperature differently influenced the decolorization of the dyes. For example, when varying it from 20°C to 50°C , the increase in the $1/m$ values was much greater with Chromotrope 2R than with Methyl Orange, both evaluated under the same reaction condition. When considering the Bismarck Brown Y dye, the increase in temperature had less influence on its decolorization in the presence of Salicylic Acid compared to the reducers Gallic Acid and Hydroquinone. On the other hand, the effect of temperature was more similar when comparing Cysteine and Ascorbic Acid to decolorize Safranin T.

When considering the different reaction systems, the following order was observed: $\text{Fe}^{3+}/\text{H}_2\text{O}_2/\text{reducer} < \text{Fe}^{2+}/\text{H}_2\text{O}_2 < \text{Fe}^{2+}/\text{H}_2\text{O}_2/\text{reducer}$. However, decolorization experiments involving Bismarck Brown Y dye and mediated by Gallic Acid or Hydroquinone did not follow this order, as the values of $1/m$ referring to the $\text{Fe}^{3+}/\text{H}_2\text{O}_2/\text{reducer}$ system were greater than those found for $\text{Fe}^{2+}/\text{H}_2\text{O}_2$. For Chromotrope 2R, the three reaction systems had similar behavior.

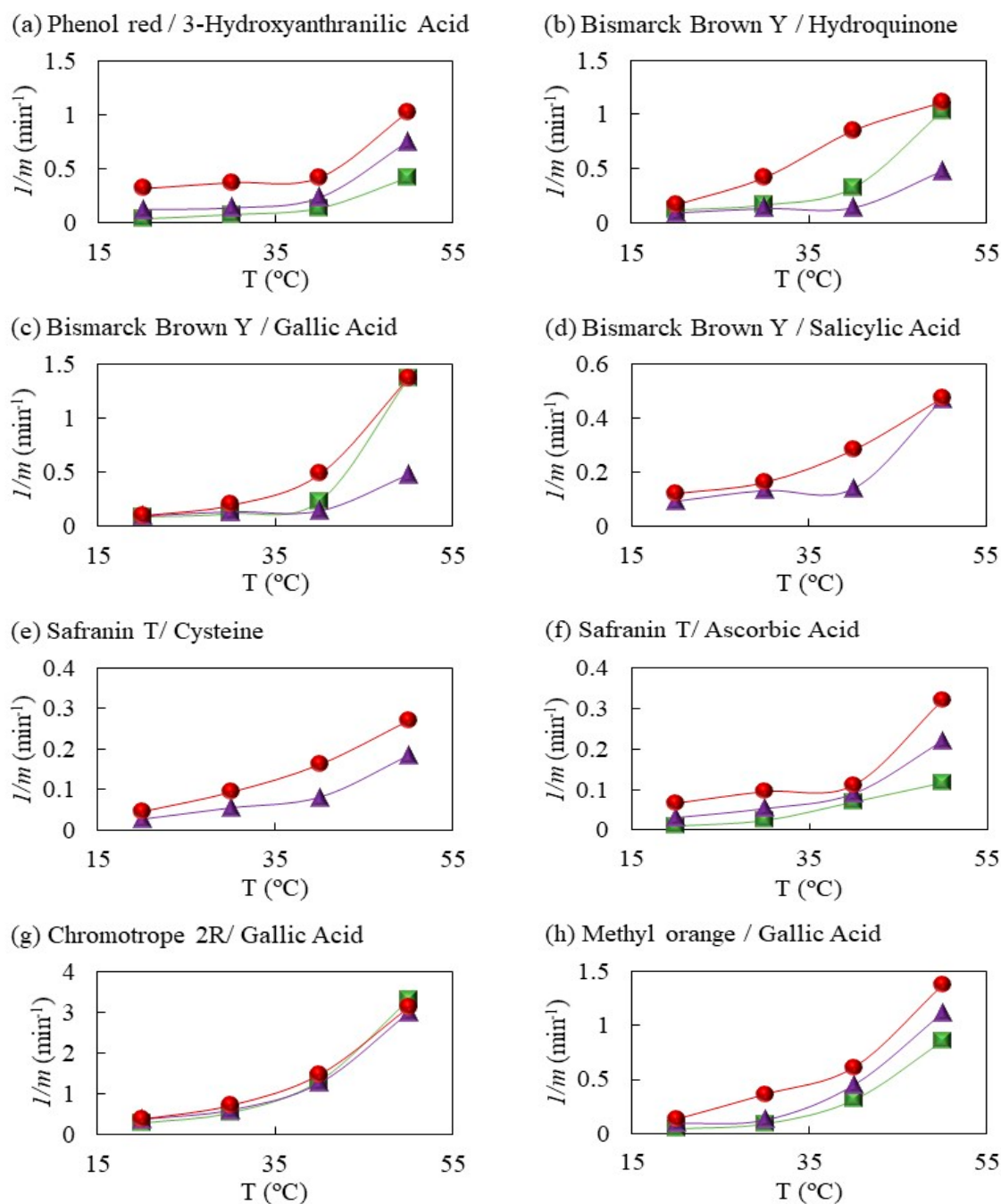


Figure 3. Effect of temperature on $1/m$ values from the decolorization of dyes by Fenton processes mediated by different reducing compounds. Reaction systems: $\text{Fe}^{2+}/\text{H}_2\text{O}_2$ (\blacktriangle), $\text{Fe}^{2+}/\text{H}_2\text{O}_2/\text{reducer}$ (\bullet) and $\text{Fe}^{3+}/\text{H}_2\text{O}_2/\text{reducer}$ (\blacksquare).

The parity plot between the experimental and the predicted data can clarify if a kinetic model is suitable in describing a reaction system [38–40]. Figures S1–S5 (available in the Supplementary Materials) show the parity plots between the experimental data of decolorization at different temperatures and the results predicted through the equations obtained from the BMG kinetic model. For most of the reaction systems, the predictions of the models are in good agreement with the respective experimental results. Only one R^2 value was slightly lower than 0.8, which is the parity graph referring to Safranin T decolorization by $\text{Fe}^{2+}/\text{H}_2\text{O}_2/\text{Ascorbic Acid}$ system. In this way, through the analysis of parity plots, the BMG model was adequate to describe the decolorization of the dyes by Fenton processes.

2.2. E_a Calculation

Using Arrhenius plots (Figure 4), which relate the values of $1/m$ and the inverse of the temperatures, the E_a values of all reaction systems were calculated (Figures 5–9). It is noteworthy that four temperature values were evaluated, as this quantity is commonly used to calculate E_a in Fenton processes [6,7,34,41]. Almost all values of R^2 were high (most above 0.8), regardless of the dye and the reaction system. This indicates that, through Arrhenius plots, data from the BMG model can be used to calculate E_a . For comparison purposes, the E_a values obtained in previous our works, using first- or second-order kinetic constants, have been included in Figures 5–9.

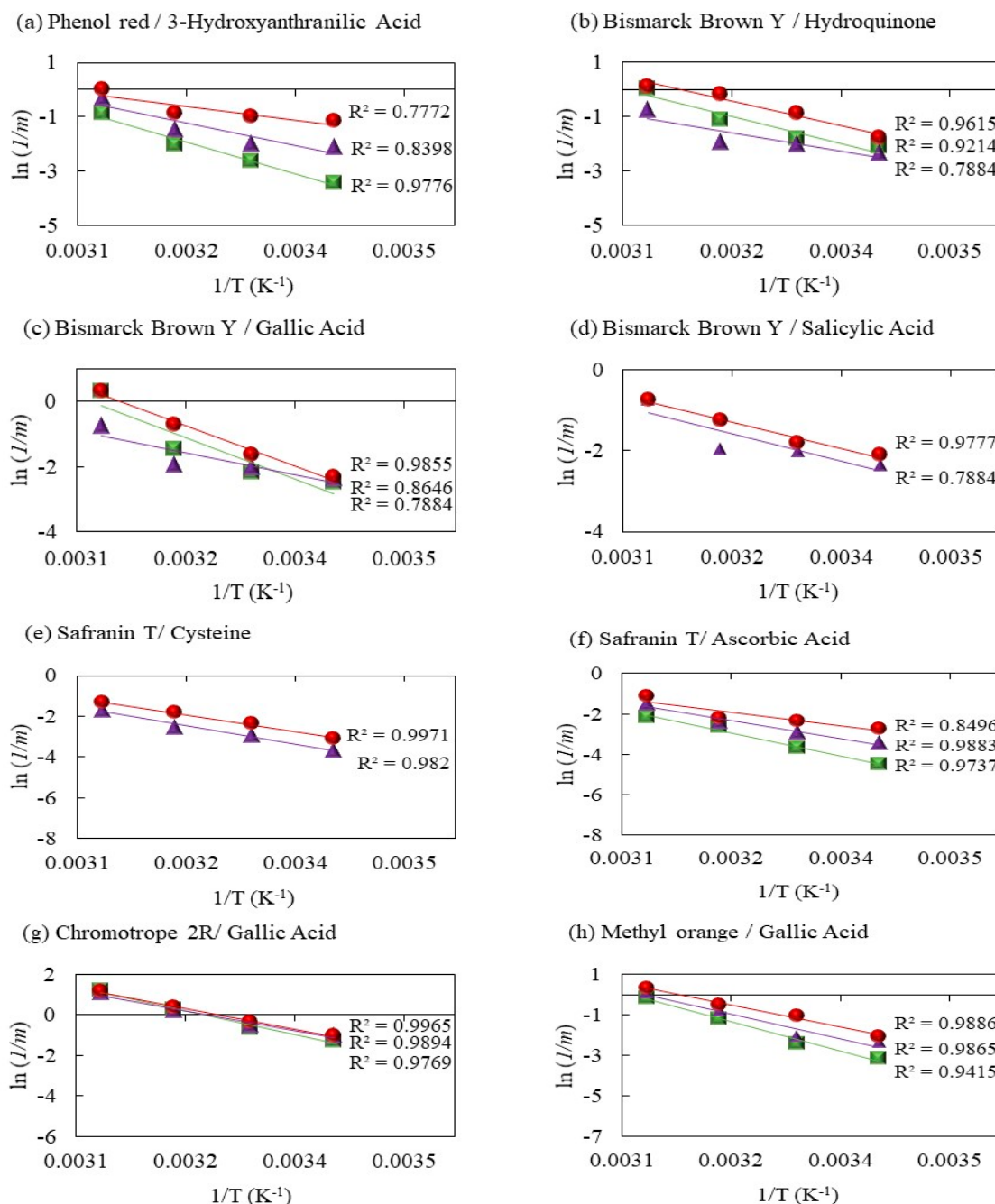


Figure 4. Arrhenius plots for the data of decolorization of different dyes by Fenton processes mediated by different reducing compounds. Systems: $\text{Fe}^{2+}/\text{H}_2\text{O}_2$ (▲), $\text{Fe}^{2+}/\text{H}_2\text{O}_2/\text{reducer}$ (●) and $\text{Fe}^{3+}/\text{H}_2\text{O}_2/\text{reducer}$ (■).

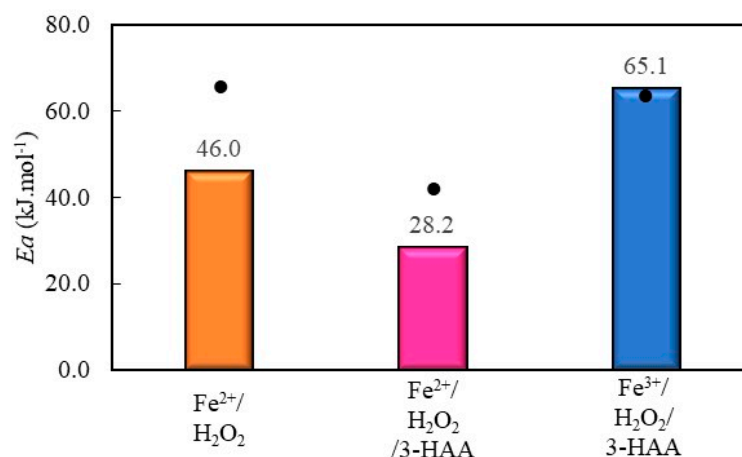


Figure 5. E_a values from Phenol Red decolorization via Fenton processes. Reaction conditions: $[\text{Fe}] = 30 \mu\text{mol L}^{-1}$; $[\text{H}_2\text{O}_2] = 300 \mu\text{mol L}^{-1}$; $[\text{dye}] = 30 \mu\text{mol L}^{-1}$; $[\text{3-HAA—3-Hydroxyanthranilic Acid}] = 10 \mu\text{mol L}^{-1}$; $\text{pH} = 2.5\text{--}3.0$. Bars: E_a values corresponding to the BMG model and calculated in the present study; dots: E_a values corresponding to the first-order reaction model based on past published data [20].

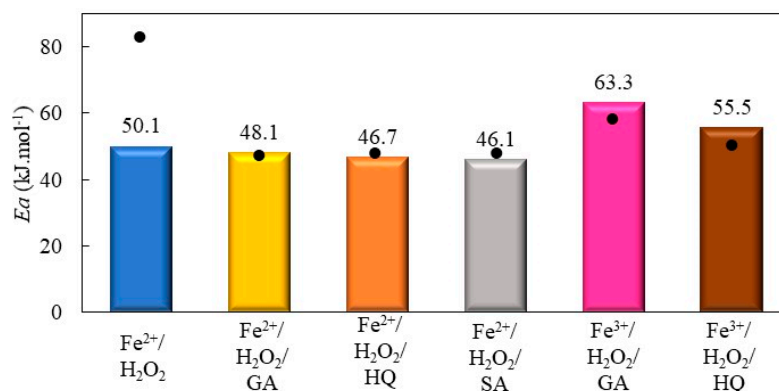


Figure 6. E_a values from Bismarck Brown Y decolorization via Fenton processes. Reaction conditions: $[\text{Fe}] = 30 \mu\text{mol L}^{-1}$; $[\text{H}_2\text{O}_2] = 450 \mu\text{mol L}^{-1}$; $[\text{dye}] = 30 \mu\text{mol L}^{-1}$; $[\text{reducer}] = 10 \mu\text{mol L}^{-1}$; $\text{pH} = 2.5\text{--}3.0$. Compounds evaluated: GA—Gallic Acid; HQ—Hydroquinone; SA—Salicylic Acid. Bars: E_a values corresponding to the BMG model and calculated in the present study; Dots: E_a values corresponding to the second-order reaction model based on past published data [24].

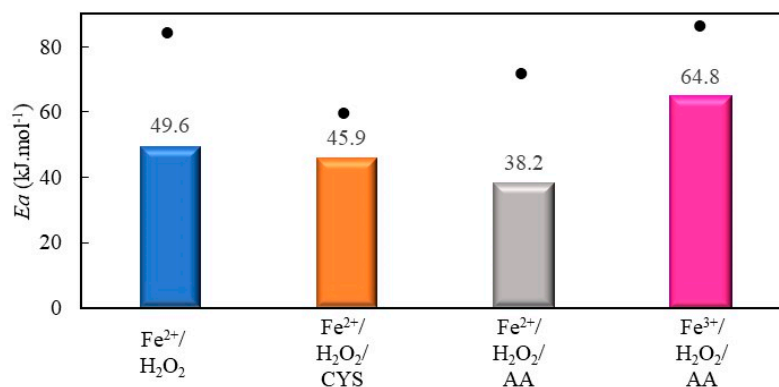


Figure 7. E_a values from Safranin T decolorization via Fenton processes. Reaction conditions: $[\text{Fe}] = 30 \mu\text{mol L}^{-1}$; $[\text{H}_2\text{O}_2] = 300 \mu\text{mol L}^{-1}$; $[\text{dye}] = 40 \mu\text{mol L}^{-1}$; $[\text{reducer}] = 10 \mu\text{mol L}^{-1}$; $\text{pH} = 2.5\text{--}3.0$. Reducers evaluated: CYS—Cysteine; AA—Ascorbic Acid. Bars: E_a values corresponding to the BMG model and calculated in the present study; dots: E_a values corresponding to the first-order reaction model based on past published data [22,23].

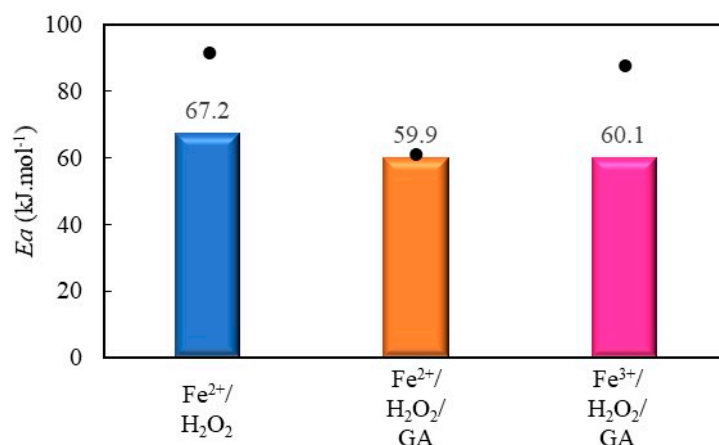


Figure 8. E_a values from decolorization of Methyl Orange via Fenton processes. Reaction conditions: $[\text{Fe}] = 30 \mu\text{mol L}^{-1}$; $[\text{H}_2\text{O}_2] = 450 \mu\text{mol L}^{-1}$; $[\text{dye}] = 40 \mu\text{mol L}^{-1}$; $[\text{GA—Gallic Acid}] = 10 \mu\text{mol L}^{-1}$; $\text{pH} = 2.5\text{--}3.0$. Bars: E_a values corresponding to the BMG model and calculated in the present study; dots: E_a values corresponding to the first-order reaction model based on past published data [21].

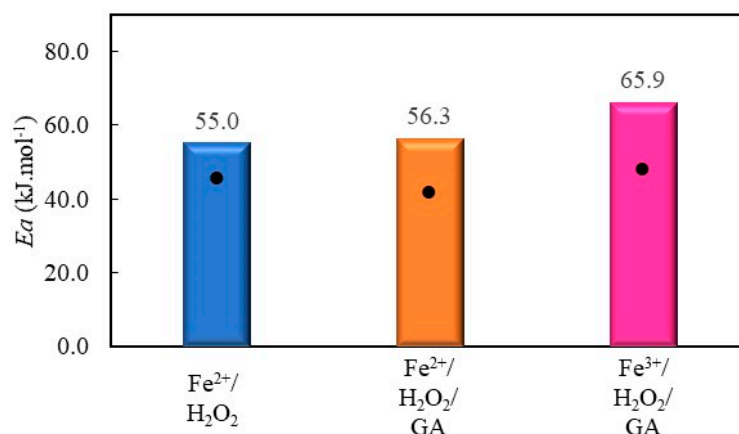


Figure 9. E_a values from Chromotrope 2R decolorization via Fenton processes. Reaction conditions: $[\text{Fe}] = 30 \mu\text{mol L}^{-1}$; $[\text{H}_2\text{O}_2] = 450 \mu\text{mol L}^{-1}$; $[\text{dye}] = 40 \mu\text{mol L}^{-1}$; $[\text{GA—Gallic Acid}] = 10 \mu\text{mol L}^{-1}$; $\text{pH} = 2.5\text{--}3.0$. Bars: E_a values corresponding to the BMG model and calculated in the present study; dots: E_a values corresponding to the second-order reaction model based on past published data [21].

2.2.1. Phenol Red Decolorization by Fenton Processes Mediated by 3-Hydroxyanthranilic Acid

The 3-Hydroxyanthranilic Acid (3-HAA) is a metabolite produced by the wood-decomposing fungus *Picnoporus cinnabarinus* [42]. Its pro-oxidant effect may be linked to its Fe^{3+} -reducing activity [10], consequently increasing the formation of hydroxyl radicals. When evaluating Phenol Red as a target pollutant, E_a values referring to Fenton processes are shown in Figure 5.

The E_a values from Phenol Red decolorization followed this order: $\text{Fe}^{3+}/\text{H}_2\text{O}_2/3\text{-HAA} > \text{Fe}^{2+}/\text{H}_2\text{O}_2 > \text{Fe}^{2+}/\text{H}_2\text{O}_2/3\text{-HAA}$. The addition of 3-HAA promoted a decrease in E_a by 39% when comparing the two last reaction systems. When considering data of E_a obtained with the first-order model [20], a lower difference was observed, 28%. Highlighting the contrast in E_a from $1/m$ values, the $\text{Fe}^{3+}/\text{H}_2\text{O}_2/3\text{-HAA}$ system exhibited the highest one, surpassing the values for $\text{Fe}^{2+}/\text{H}_2\text{O}_2$ by 30% and $\text{Fe}^{2+}/\text{H}_2\text{O}_2/3\text{-HAA}$ by 57%.

2.2.2. Decolorization of Bismarck Brown Y by Fenton Processes Mediated by Hydroquinone, Gallic Acid, and Salicylic Acid

When evaluating the decolorization of the Bismarck Brown Y dye by Fenton processes, three compounds were tested, namely Hydroquinone, Gallic Acid, or Salicylic Acid. It is important to mention that Salicylic Acid is not a reducer of Fe^{3+} , but it can be converted

into dihydroxylated reducers (2,5-dihydroxybenzoic acid, 2,3-dihydroxybenzoic acid, and catechol) by HO^\bullet radicals during the reactions [14]. Figure S6 shows the Salicylic Acid being converted into intermediates, which react with Fe^{3+} and then are converted into their respective quinones. The simplified mechanisms involving reactions between Fenton reagents and Hydroquinone or Gallic acid are shown in Figure S7 and Figure S8, respectively.

As shown in Figure 6, the three compounds decreased E_a when comparing $\text{Fe}^{2+}/\text{H}_2\text{O}_2$ and $\text{Fe}^{2+}/\text{H}_2\text{O}_2/\text{reducer}$ systems. Salicylic Acid decreased the E_a by 8%, while Hydroquinone decreased by 7%. In turn, the addition of Gallic Acid reduced E_a by less than 5%. When the second-order rate constants were used in previous our study [24], this percentage decrease in E_a was much more evident. In the presence of Gallic Acid or Hydroquinone, $\text{Fe}^{3+}/\text{H}_2\text{O}_2/\text{reducer}$ system exhibited higher E_a from $1/m$ values, surpassing $\text{Fe}^{2+}/\text{H}_2\text{O}_2$ and $\text{Fe}^{2+}/\text{H}_2\text{O}_2/\text{reducer}$ by up to 24%.

2.2.3. Decolorization of Safranin T by Fenton Processes Mediated by Cysteine and Ascorbic Acid

The E_a values obtained from the decolorization of Safranin T are shown in Figure 7. Unlike other studies, two natural non-phenolic reducers were evaluated to decolorize this dye: Cysteine and Ascorbic Acid. Cysteine is an amino acid generally produced through the hydrolysis of keratin [43], and has the ability to reduce Fe^{3+} due to the presence of a sulfhydryl group ($-\text{SH}$) in its molecule. The reaction between Fe^{3+} and Cysteine results in Fe^{2+} and Cystine. The latter may undergo reaction with HO^\bullet to regenerate Cysteine or be converted into Cystic acid [44]. Ascorbic Acid, also known as vitamin C, is found in many vegetables, although it is produced industrially from glucose [45]. At pH 3.0, Ascorbic Acid is partly found as ascorbate monoanion (AA^-), which undergoes a two-step oxidation to yield dehydroascorbic acid. Besides AA^- , other intermediates (ascorbyl radical; $\text{AA}^{\bullet-}$) actively reduce Fe^{3+} to Fe^{2+} , catalyzing the conversion of H_2O_2 to HO^\bullet radical through the Fenton reaction [46]. The simplified mechanisms involving reactions between the two reducers aforementioned and Fenton reagents are shown in Figure S9 and Figure S10, respectively.

As with other dyes, $\text{Fe}^{2+}/\text{H}_2\text{O}_2/\text{reducer}$ system showed lower E_a than $\text{Fe}^{2+}/\text{H}_2\text{O}_2$. The Ascorbic Acid promoted a decrease in E_a by 23%, while the Cysteine only decreased by 7%. This suggests that there may be distinct interactions between Fe ions and the two reducing compounds studied. This explanation also applies to Bismarck Brown Y decolorization influenced by three compounds (Section 2.2.2). When comparing the systems in the presence of Ascorbic Acid, the E_a value for the $\text{Fe}^{3+}/\text{H}_2\text{O}_2/\text{reducer}$ system was 69% higher than $\text{Fe}^{2+}/\text{H}_2\text{O}_2/\text{reducer}$. Similar to Phenol Red and Bismarck Brown Y (Sections 2.2.1 and 2.2.2, respectively), $\text{Fe}^{3+}/\text{H}_2\text{O}_2/\text{reducer}$ system had the higher energy barrier to decolorize Safranin T.

In general, the E_a values previously calculated by the first-order reaction model were higher than those calculated by the BMG model. Furthermore, there was an inversion in the order of E_a values between the reaction systems with reducers. For example, the order of values of E_a from k_1 of the previous studies was $\text{Fe}^{3+}/\text{H}_2\text{O}_2/\text{Ascorbic Acid} > \text{Fe}^{2+}/\text{H}_2\text{O}_2 > \text{Fe}^{2+}/\text{H}_2\text{O}_2/\text{Ascorbic Acid} > \text{Fe}^{2+}/\text{H}_2\text{O}_2/\text{Cysteine}$, while when considering the $1/m$, the order was changed to $\text{Fe}^{3+}/\text{H}_2\text{O}_2/\text{Ascorbic Acid} > \text{Fe}^{2+}/\text{H}_2\text{O}_2 > \text{Fe}^{2+}/\text{H}_2\text{O}_2/\text{Cysteine} > \text{Fe}^{2+}/\text{H}_2\text{O}_2/\text{Ascorbic Acid}$.

2.2.4. Decolorization of Methyl Orange by Fenton Processes Mediated by Gallic Acid

Gallic Acid is a polyphenolic reducer extracted from plants and has been one of the most evaluated in the literature as a pro-oxidant in Fenton processes, as recently reviewed by Lima et al. [47]. In addition to the Bismarck Brown Y dye (Section 2.2.2), Gallic Acid was evaluated in the decolorization of two other azo dyes: Methyl Orange and Chromotrope 2R.

The E_a values for the decolorization of Methyl Orange are shown in Figure 8. Comparing the $\text{Fe}^{2+}/\text{H}_2\text{O}_2$ and $\text{Fe}^{2+}/\text{H}_2\text{O}_2/\text{reducer}$ systems, the percentage of decrease in E_a was 11% due to the addition of Gallic Acid. Curiously, E_a values were similar for

the $\text{Fe}^{2+}/\text{H}_2\text{O}_2/\text{GA}$ and $\text{Fe}^{3+}/\text{H}_2\text{O}_2/\text{GA}$ systems. Notably, the reduction in E_a was more pronounced when employing the conventional first-order reaction model for the $\text{Fe}^{2+}/\text{H}_2\text{O}_2/\text{GA}$ system in relation to the others.

2.2.5. Decolorization of Chromotrope 2R by Gallic Acid-Mediated Fenton Processes

The E_a values for the decolorization of Chromotrope 2R are shown in Figure 9. Unlike other dyes, there was practically no significant change in E_a values regarding $\text{Fe}^{2+}/\text{H}_2\text{O}_2$ and $\text{Fe}^{2+}/\text{H}_2\text{O}_2/\text{GA}$. $\text{Fe}^{3+}/\text{H}_2\text{O}_2/\text{GA}$ exhibited the highest E_a value among the systems, surpassing $\text{Fe}^{2+}/\text{H}_2\text{O}_2$ and $\text{Fe}^{2+}/\text{H}_2\text{O}_2/\text{GA}$ by 17% and 15%, respectively. Except for Methyl Orange (Section 2.2.4), the $\text{Fe}^{3+}/\text{H}_2\text{O}_2/\text{reducer}$ system had the higher energy barrier to decolorize the dyes.

It is important to mention that in the previous study, when calculating E_a using data from the second-order model [21], no variation in E_a was reported when Gallic Acid was added. This result can possibly be attributed to the greater susceptibility of Chromotrope 2R to being decolorized by free radicals, regardless of the presence of Gallic Acid.

Considering that the concentrations of the reagents in the experiments to decolorize each dye are not similar, the values of the $[\text{Fe}]:[\text{H}_2\text{O}_2]$ ratio are different. Consequently, the production of HO^\bullet radical is influenced, interfering in the degradation of a target pollutant by Fenton processes [6,16]. In addition, dyes may exhibit different susceptibility to HO^\bullet radicals. This aspect can be attributed to the different reactivity of its chromosphere groups and other non-chromophore sites present in their molecules [48,49]. Therefore, even if the dyes were evaluated under the same reaction condition, the E_a values would differ between them. For example, regardless of the reaction kinetic model, E_a from decolorization of Chromotrope 2R was lower than Methyl Orange.

Comparing kinetic models and their constants used to calculate E_a , all $1/m$ values were greater than those for k_1 and k_2 , when the three models fitted well the same experimental data in our previous works. Studies developed by other research groups also observed higher values of $1/m$ compared to k_1 [27,29,30]. Regardless of the E_a values being different based on the rate constants from three kinetic models, it was possible to verify that all Fe^{3+} -reducing compounds (in addition to Salicylic Acid) presented pro-oxidant behavior to degrade different dyes through Fenton processes.

3. Materials and Methods

Decolorization tests were carried out in triplicate, in the dark, and without agitation. The reactions were carried out in quartz cuvettes with a reaction volume of 2 mL containing a target dye, H_2O_2 , FeSO_4 or $\text{Fe}(\text{NO}_3)_3$, H_2SO_4 (to adjust the pH in the ideal range between 2.5 and 3.0), and a reducer. The solutions were kept in a water bath for 10 min to reach the designed temperature (20, 30, 40, and 50 °C), and then Fe ions were added to start the reactions. This time interval also demonstrated that there was no decolorization of any of the dyes due to the unique effect of temperature. The different dyes and reducers, in addition to the concentrations of all reagents, are shown in Table 1 and additional details can be obtained from previous studies.

Dye decolorization was monitored on a spectrophotometer (NI 1800UV, Nova Instruments, Piracicaba, SP, Brazil) by decreasing absorbance at the characteristic maximum wavelength (λ_{max}) of each dye under the reaction conditions studied. The reference solution in the equipment contained all reagents except the dye and iron ions. Analytical curves were prepared to determine the residual concentration of the dyes. Controls involving the reagents separately (including only the reducers, Fe salts, or H_2O_2) were conducted in our previous studies, and did not present decolorization.

Table 1. Concentration of reagents evaluated in dye degradation tests via Fenton processes.

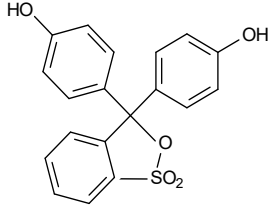
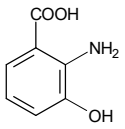
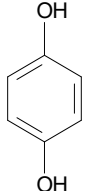
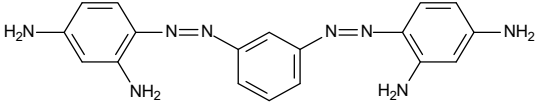
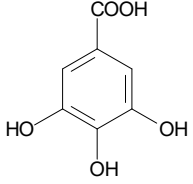
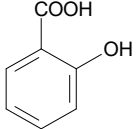
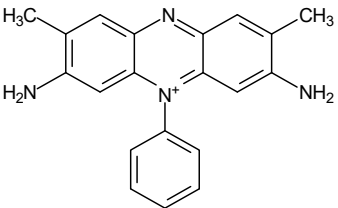
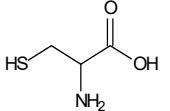
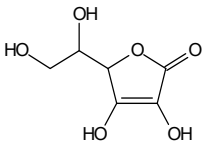
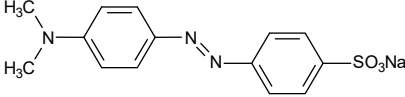
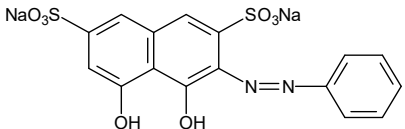
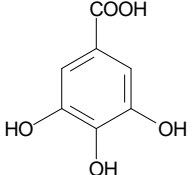
[Dye]	Dye's Chemical Structure	λ_{\max} (nm)	$[\text{H}_2\text{O}_2]$ ($\mu\text{mol}\cdot\text{L}^{-1}$)	$[\text{FeSO}_4]$ or $[\text{Fe}(\text{NO}_3)_3]$ ($\mu\text{mol}\cdot\text{L}^{-1}$)	$[\text{H}_2\text{SO}_4]$ ($\text{mmol}\cdot\text{L}^{-1}$)	[Reducer]	Reducer's Chemical Structure	Reference
$30 \mu\text{mol}\cdot\text{L}^{-1}$ Phenol red		435	300	30	1	$10 \mu\text{mol}\cdot\text{L}^{-1}$ 3-Hydroxyanthranilic Acid		[20]
						$10 \mu\text{mol}\cdot\text{L}^{-1}$ Hydroquinone		
$30 \mu\text{mol}\cdot\text{L}^{-1}$ Bismarck Brown Y		450	450	30	1	$10 \mu\text{mol}\cdot\text{L}^{-1}$ Gallic Acid		[24]
						$10 \mu\text{mol}\cdot\text{L}^{-1}$ Salicylic Acid		

Table 1. Cont.

[Dye]	Dye's Chemical Structure	λ_{\max} (nm)	$[\text{H}_2\text{O}_2]$ ($\mu\text{mol}\cdot\text{L}^{-1}$)	$[\text{FeSO}_4]$ or $[\text{Fe}(\text{NO}_3)_3]$ ($\mu\text{mol}\cdot\text{L}^{-1}$)	$[\text{H}_2\text{SO}_4]$ ($\text{mmol}\cdot\text{L}^{-1}$)	[Reducer]	Reducer's Chemical Structure	Reference
40 $\mu\text{mol}\cdot\text{L}^{-1}$ Safranin T		519	300	30	1	10 $\mu\text{mol}\cdot\text{L}^{-1}$ Cysteine		[22]
						10 $\mu\text{mol}\cdot\text{L}^{-1}$ Ascorbic Acid		[23]
40 $\mu\text{mol}\cdot\text{L}^{-1}$ Methyl Orange		508						
40 $\mu\text{mol}\cdot\text{L}^{-1}$ Chromotrope 2R		513	450	30	1	10 $\mu\text{mol}\cdot\text{L}^{-1}$ Gallic Acid		[21]

From the decolorization data over 60 min, a kinetic study was carried out based on the BMG model (Equation (6)) [23]. Using the values of $1/m$ at different temperatures, the Ea values were calculated for the decolorization reactions of the different dyes using the linearized Arrhenius equation (substituting k for $1/m$), as shown in Equation (10) [33].

$$\ln\left(\frac{1}{m}\right) = \ln(A) - \frac{Ea}{R \cdot T} \quad (10)$$

where A is the frequency (min^{-1}); Ea is the activation energy ($\text{J} \cdot \text{mol}^{-1}$); R is the ideal gas constant ($8.314 \text{ J} \cdot \text{mol}^{-1} \cdot \text{K}^{-1}$); and T is the absolute temperature (K). The graph $\ln(1/m)$ vs. $1/T$ has allowed calculating the activation energy values from its slope.

4. Conclusions

Through the kinetic study using the BMG model, it can be noted that the values of the initial reaction rates ($1/m$) obtained from the decolorization reactions of different dyes using Fenton processes ($\text{Fe}^{2+}/\text{H}_2\text{O}_2$, $\text{Fe}^{2+}/\text{H}_2\text{O}_2/\text{reducer}$, and $\text{Fe}^{3+}/\text{H}_2\text{O}_2/\text{reducer}$) were increased in the presence of Fe^{3+} -reducing organic compounds. For almost all dyes evaluated, the activation energy (Ea) calculated from the $1/m$ values showed that the energy barrier of reactions initially containing Fe^{2+} was lower due to addition of reducers. Except for one of the dyes, Methyl Orange, the $\text{Fe}^{3+}/\text{H}_2\text{O}_2/\text{reducer}$ system had the higher energy barrier to decolorize the dyes. Compared to Ea values from k_1 or k_2 data (from previous our works), the Ea values obtained from $1/m$ showed less differentiation between the reaction systems in the presence or absence of reducers. Although Ea values obtained from conventional kinetic models demonstrated more evident effect of reducers, the BMG model can be indicated as a complementary analysis to verify the pro-oxidant behavior of these compounds in Fenton processes.

Supplementary Materials: The following supporting information can be downloaded at: <https://www.mdpi.com/article/10.3390/catal14040273/s1>, Figure S1. Parity plots of Phenol Red decolorization data by Fenton processes in the absence (control) or presence of 3-Hydroxyanthranilic Acid as reducer. Reaction systems: $\text{Fe}^{2+}/\text{H}_2\text{O}_2$ (\blacktriangle), $\text{Fe}^{2+}/\text{H}_2\text{O}_2/\text{reducer}$ (\bullet) and $\text{Fe}^{3+}/\text{H}_2\text{O}_2/\text{reducer}$ (\blacksquare). Figure S2. Parity plots of Bismarck Brown Y decolorization data by Fenton processes in the absence (control) or presence of Hydroquinone, Gallic Acid or Salicylic Acid. Reaction systems: $\text{Fe}^{2+}/\text{H}_2\text{O}_2$ (\blacktriangle), $\text{Fe}^{2+}/\text{H}_2\text{O}_2/\text{reducer}$ (\bullet) and $\text{Fe}^{3+}/\text{H}_2\text{O}_2/\text{reducer}$ (\blacksquare). Figure S3. Parity plots of Safranin T decolorization data by Fenton processes in the absence (control) or presence of Cysteine or Ascorbic Acid as reducers. Reaction systems: $\text{Fe}^{2+}/\text{H}_2\text{O}_2$ (\blacktriangle), $\text{Fe}^{2+}/\text{H}_2\text{O}_2/\text{reducer}$ (\bullet) and $\text{Fe}^{3+}/\text{H}_2\text{O}_2/\text{reducer}$ (\blacksquare). Figure S4. Parity plots of Chromotrope R decolorization data by Fenton processes in the absence (control) or presence of Gallic Acid as reducer. Reaction systems: $\text{Fe}^{2+}/\text{H}_2\text{O}_2$ (\blacktriangle), $\text{Fe}^{2+}/\text{H}_2\text{O}_2/\text{reducer}$ (\bullet) and $\text{Fe}^{3+}/\text{H}_2\text{O}_2/\text{reducer}$ (\blacksquare). Figure S5. Parity plots of Methyl Orange decolorization data by Fenton processes in the absence (control) or presence of Gallic Acid as reducer. Reaction systems: $\text{Fe}^{2+}/\text{H}_2\text{O}_2$ (\blacktriangle), $\text{Fe}^{2+}/\text{H}_2\text{O}_2/\text{reducer}$ (\bullet) and $\text{Fe}^{3+}/\text{H}_2\text{O}_2/\text{reducer}$ (\blacksquare). Figure S6. Fe^{3+} -reducing intermediates formed from Salicylic Acid hydroxylation. (A) 2,5-dihydroxybenzoic acid, (B) 2,3-dihydroxybenzoic acid, (C) catechol; reactions between Fe^{3+} ions and intermediates and products of its oxidation (quinones, carboxylic acids, CO_2 , H_2O). Figure S7. Reactions between Fe ions, HO_2^\bullet radical, Hydroquinone, and its intermediates. Figure S8. Reduction of Fe^{3+} ions by Gallic Acid (GA) and its oxidized intermediates. The regenerated Fe^{2+} ions can react with H_2O_2 to generate more HO^\bullet radicals via Fenton reaction. Figure S9. Reactions between Fenton reagents (Fe ions, H_2O_2), Cysteine, and their intermediates (Cystine, Cystic acid), HO^\bullet radical, and organic pollutants eventually present in the solution. Figure S10. Reactions between Fenton reagents (Fe ions, H_2O_2), Ascorbic Acid (AA), and their intermediates (AA^- —ascorbate monoanion; AA^\bullet —semidehydroascorbate; $\text{AA}^{\bullet-}$ —ascorbyl radical; DHA—dehydroascorbic acid), HO^\bullet radical, and degradation of organic pollutants eventually present in the solution. Ref. [50] is cited in Supplementary Materials.

Author Contributions: Conceptualization, A.A.; formal analysis, M.D.N.R., J.P.P.L. and A.A.; investigation, M.D.N.R., J.P.P.L. and A.A.; data curation, M.D.N.R., J.P.P.L. and A.A.; writing—original draft preparation, M.D.N.R., J.P.P.L. and A.A.; writing—review, supervision and editing, A.A. All authors have read and agreed to the published version of the manuscript.

Funding: This research was funded by Brazilian Agencies for Scientific and Technological Development: Fundação de Amparo à Pesquisa do Estado de Minas Gerais (Fapemig, project number APQ-01898-17), Conselho Nacional de Desenvolvimento Científico e Tecnológico (CNPq), and Coordenação de Aperfeiçoamento de Ensino Superior (CAPES). The English grammar review of this article was funded by the Institute of Natural Resources of the Federal University of Itajubá.

Data Availability Statement: All data generated or analyzed during this study are included in this article and previous articles published by our group: <https://doi.org/10.1007/s11270-021-05258-1>; <https://doi.org/10.1007/s11270-021-05258-1>; <https://doi.org/10.1080/09593330.2020.1776402>; <https://doi.org/10.1016/j.psep.2022.10.083>; and <https://doi.org/10.1080/09593330.2021.1921855>.

Conflicts of Interest: The authors declare no conflict of interest.

References

1. Ramos, M.D.N.; Lima, J.P.P.; Aquino, S.F.; Aguiar, A. A critical analysis of the alternative treatments applied to effluents from Brazilian textile industries. *J. Water Process Eng.* **2021**, *43*, 102273. [CrossRef]
2. Katheresan, V.; Kannedo, J.; Lau, S.Y. Efficiency of various recent wastewater dye removal methods: A review. *J. Environ. Chem. Eng.* **2018**, *6*, 4676–4697. [CrossRef]
3. Kastanek, F.; Spacilova, M.; Krystynik, P.; Dlaskova, M.; Solcova, O. Fenton reaction—unique but still mysterious. *Processes* **2023**, *11*, 432. [CrossRef]
4. Holkar, C.R.; Jadhav, A.J.; Pinjari, D.V.; Mahamuni, N.M.; Pandit, A.B. A critical review on textile wastewater treatments: Possible approaches. *J. Environ. Manag.* **2016**, *182*, 351–366. [CrossRef] [PubMed]
5. Al-Tohamy, R.; Ali, S.S.; Li, F.; Okasha, K.M.; Mahmoud, Y.A.G.; Elsamahy, T.; Jiao, H.; Fu, Y.; Sun, J. A critical review on the treatment of dye-containing wastewater: Ecotoxicological and health concerns of textile dyes and possible remediation approaches for environmental safety. *Ecotoxicol. Environ. Saf.* **2022**, *231*, 113160. [CrossRef] [PubMed]
6. Argun, M.E.; Karatas, M. Application of Fenton process for decolorization of Reactive Black 5 from synthetic wastewater: Kinetics and thermodynamics. *Environ. Prog. Sustain. Energy* **2011**, *30*, 540–548. [CrossRef]
7. Tony, M.A.; Mansour, S.A. Removal of the commercial reactive dye Procion Blue MX-7RX from real textile wastewater using the synthesized Fe₂O₃ nanoparticles at different particle sizes as a source of Fenton's reagent. *Nanoscale Adv.* **2019**, *1*, 1362. [CrossRef] [PubMed]
8. Li, Y.; Cheng, H. Chemical kinetic modeling of organic pollutant degradation in Fenton and solar photo-Fenton processes. *J. Taiwan Inst. Chem. Eng.* **2021**, *123*, 175–184. [CrossRef]
9. Kamenická, B.; Weidlich, T. A Comparison of different reagents applicable for destroying halogenated anionic textile dye Mordant Blue 9 in polluted aqueous streams. *Catalysts* **2023**, *13*, 460. [CrossRef]
10. Aguiar, A.; Ferraz, A. Fe³⁺- and Cu²⁺-reduction by phenol derivatives associated with Azure B degradation in Fenton-like reactions. *Chemosphere* **2007**, *66*, 947–954. [CrossRef]
11. Zhang, M.H.; Dong, H.; Zhao, L.; Wang, D.X.; Meng, D. A review on Fenton process for organic wastewater treatment based on optimization perspective. *Sci. Total Environ.* **2019**, *670*, 110–121. [CrossRef]
12. Ramos, M.D.N.; Santana, C.S.; Velloso, C.C.V.; Silva, A.H.M.; Magalhães, F.; Aguiar, A. A review on the treatment of textile industry effluents through Fenton processes. *Process Saf. Environ. Prot.* **2021**, *155*, 366–386. [CrossRef]
13. Bello, M.M.; Abdul, R.; Abdul, A.; Asghar, A. A review on approaches for addressing the limitations of Fenton oxidation for recalcitrant wastewater treatment. *Process Saf. Environ. Prot.* **2019**, *126*, 119–140. [CrossRef]
14. Chen, F.; Ma, W.; He, J.; Zhao, J. Fenton degradation of malachite green catalyzed by aromatic additives. *J. Phys. Chem. A* **2002**, *106*, 9485–9490. [CrossRef]
15. Pan, Y.; Qin, R.; Hou, M.; Xue, J.; Zhou, M.; Xu, L.; Zhang, Y. The interactions of polyphenols with Fe and their application in Fenton/Fenton-like reactions. *Sep. Purif. Technol.* **2022**, *300*, 121831. [CrossRef]
16. Farooq, U.; Wang, F.; Shang, J.; Shahid, M.Z.; Akram, W.; Wang, X. Heightening effects of cysteine on degradation of trichloroethylene in Fe³⁺/SPC process. *Chem. Eng. J.* **2023**, *454*, 139996. [CrossRef]
17. Han, X.; Wang, N.; Zhang, W.; Liu, X.; Yu, Q.; Lei, J.; Zhou, L.; Xiu, G. Ascorbic acid promoted sulfamethoxazole degradation in MIL-88B (Fe)/H₂O₂ Fenton-like system. *J. Environ. Chem. Eng.* **2023**, *11*, 109144. [CrossRef]
18. Sun, H.; Xie, G.; He, D.; Zhang, L. Ascorbic acid promoted magnetite Fenton degradation of alachlor: Mechanistic insights and kinetic modeling. *Appl. Catal. B Environ.* **2020**, *267*, 118383. [CrossRef]
19. Yuan, Y.; Chen, S.; Yao, B.; Chen, A.; Peng, L.; Luo, S.; Zhou, Y. Fe³⁺-cysteine enhanced persulfate Fenton-like process for quinclorac degradation: A wide pH tolerance and reaction mechanism. *Environ. Res.* **2023**, *224*, 115447. [CrossRef] [PubMed]
20. Santana, C.S.; Ramos, M.D.N.; Velloso, C.C.V.; Aguiar, A. Kinetic evaluation of dye decolorization by Fenton processes in the presence of 3-hydroxyanthranilic acid. *Int. J. Environ. Res. Public Health* **2019**, *16*, 1602. [CrossRef] [PubMed]

21. Tabelini, C.H.B.; Lima, J.P.P.; Aguiar, A. Gallic acid influence on azo dyes oxidation by Fenton processes. *Environ. Technol.* **2022**, *43*, 3390–3940. [[CrossRef](#)]
22. Ramos, M.D.N.; Sousa, L.A.; Aguiar, A. Effect of cysteine using Fenton processes on decolorizing different dyes: A kinetic study. *Environ. Technol.* **2022**, *43*, 70–82. [[CrossRef](#)] [[PubMed](#)]
23. Ramos, M.D.N.; Silva, G.L.S.; Lessa, T.L.; Aguiar, A. Study of kinetic parameters related to dyes oxidation in ascorbic acid-mediated Fenton processes. *Process Saf. Environ. Prot.* **2022**, *168*, 1131–1141. [[CrossRef](#)]
24. Lima, J.P.P.; Tabelini, C.H.B.; Ramos, M.D.N.; Aguiar, A. Kinetic evaluation of Bismarck Brown Y azo dye oxidation by Fenton processes in the presence of aromatic mediators. *Wat. Air Soil Pollut.* **2021**, *232*, 321. [[CrossRef](#)]
25. Chan, K.H.; Chu, W. Modeling the reaction kinetics of Fenton's process on the removal of atrazine. *Chemosphere* **2003**, *51*, 305–311. [[CrossRef](#)] [[PubMed](#)]
26. Behnajady, M.A.; Modirshahla, N.; Ghanbary, F. A kinetic model for the decolorization of C.I. Acid Yellow 23 by Fenton process. *J. Hazard Mater.* **2007**, *148*, 98–102. [[CrossRef](#)] [[PubMed](#)]
27. Tunç, S.; Duman, O.; Gürkan, T. Monitoring the decolorization of Acid Orange 8 and Acid Red 44 from aqueous solution using Fenton's reagents by online spectrophotometric method: Effect of operation parameters and kinetic study. *Ind. Eng. Chem. Res.* **2013**, *52*, 1414–1425. [[CrossRef](#)]
28. Ou, X.; Wang, C.; Zhang, F.; Sun, H.; Wu, Y. Degradation of methyl violet by Fenton's reagent: Kinetic modeling and effects of parameters. *Desalin. Water Treat.* **2013**, *51*, 2536–2542. [[CrossRef](#)]
29. León, G.; Miguel, B.; Manzanares, L.; Saavedra, M.I.; Guzmán, M.A. Kinetic study of the ultrasound effect on Acid Brown 83 dye degradation by hydrogen peroxide oxidation processes. *ChemEngineering* **2021**, *5*, 52. [[CrossRef](#)]
30. Li, F.; Choong, T.S.Y.; Soltani, S.; Abdullah, L.C.; Jamil, M.; Ain, S.N. Kinetic study of Fenton-like degradation of methylene blue in aqueous solution using calcium peroxide. *Pertanika J. Sci. Technol.* **2022**, *30*, 1087–1102. [[CrossRef](#)]
31. Kumar, J.E.; Mulai, T.; Kharmawphlang, W.; Sharan, R.N.; Sahoo, M.K. The efficiency of Fenton, Fenton/MW and UV/oxidant processes in the treatment of a mixture of higher concentrations of azo dyes. *Chem. Eng. J. Adv.* **2023**, *15*, 100515. [[CrossRef](#)]
32. Xu, H.Y.; Shi, T.N.; Wu, L.C.; Qi, S.Y. Discoloration of methyl orange in the presence of schorl and H₂O₂: Kinetics and mechanism. *Wat. Air Soil Pollut.* **2013**, *224*, 1740. [[CrossRef](#)]
33. Levenspiel, O. *Chemical Reaction Engineering*, 3rd ed.; Wiley: Hoboken, NJ, USA, 1998.
34. Santos, M.S.F.; Alves, A.; Madeira, L.M. Paraquat removal from water by oxidation with Fenton's reagent. *J. Chem. Eng.* **2011**, *175*, 279–290. [[CrossRef](#)]
35. Zazo, J.A.; Pliego, G.; Blasco, S.; Casas, J.A.; Rodriguez, J.J. Intensification of the Fenton process by increasing the temperature. *Ind. Eng. Chem. Res.* **2011**, *50*, 866–870. [[CrossRef](#)]
36. Carbajo, J.; Silveira, J.E.; Pliego, G.; Zazo, J.A.; Casas, J.A. Increasing Photo-Fenton process Efficiency: The effect of high temperatures. *Sep. Purif. Technol.* **2021**, *271*, 118876. [[CrossRef](#)]
37. Xu, H.; Yu, T.; Wang, J.; Wu, F.; Xu, A. Kinetics study of Fenton degradation of acid yellow g by online spectrometry technology. *Nat. Environ. Pollut. Technol.* **2016**, *15*, 991–996.
38. Bouasla, C.; Ismail, F.; Samar, M.E.H. Effects of operator parameters, anions and cations on the degradation of AY99 in an aqueous solution using Fenton's reagent. Optimization and kinetics study. *Int. J. Ind. Chem.* **2012**, *3*, 15. [[CrossRef](#)]
39. Arts, A.; Schmuhl, R.; de Groot, M.T.; van der Schaaf, J. Fast initial oxidation of formic acid by the Fenton reaction under industrial conditions. *J. Water Process Eng.* **2021**, *40*, 101780. [[CrossRef](#)]
40. Akram, M.; Chakrabarti, S. Mechanism and kinetic model of the oxidative degradation of Rhodamine B dye in aqueous solution by ultrasound-assisted Fenton's process. *Int. J. Environ. Waste Manag.* **2022**, *29*, 80–94. [[CrossRef](#)]
41. Kumar, V.; Pandey, N.; Dharmadhikari, S.; Ghosh, P. Degradation of mixed dye via heterogeneous Fenton process: Studies of calcination, toxicity evaluation, and kinetics. *Water Environ. Res.* **2019**, *92*, 211–221. [[CrossRef](#)] [[PubMed](#)]
42. Göçenoğlu, A.; Pazarlioglu, N. Cinnabaric acid: Enhanced production from *Pycnoporus cinnabarinus*, characterization, structural and functional properties. *Hacet. J. Biol. Chem.* **2014**, *42*, 281–290. [[CrossRef](#)]
43. Takagi, H.; Ohtsu, I. L-Cysteine metabolism and fermentation in microorganisms. In *Amino Acid Fermentation*; Yokota, A., Ikeda, M., Eds.; Springer: Tokyo, Japan, 2017; pp. 129–151.
44. Li, T.; Zhao, Z.; Wang, Q.; Xie, P.; Ma, J. Strongly enhanced Fenton degradation of organic pollutants by cysteine: An aliphatic amino acid accelerator outweighs hydroquinone analogues. *Water Res.* **2016**, *105*, 479–486. [[CrossRef](#)] [[PubMed](#)]
45. Bremus, C.; Herrmann, U.; Bringer-Meyer, S.; Sahn, H. The use of microorganisms in L-ascorbic acid production. *J. Biotech.* **2006**, *124*, 196–205. [[CrossRef](#)] [[PubMed](#)]
46. Bolobajev, J.; Trapido, M.; Goi, A. Improvement in iron activation ability of alachlor Fenton-like oxidation by ascorbic acid. *J. Chem. Eng.* **2015**, *281*, 566–574. [[CrossRef](#)]
47. Lima, J.P.P.; Tabelini, C.H.B.; Aguiar, A. A Review of gallic acid-mediated Fenton processes for degrading emerging pollutants and dyes. *Molecules* **2023**, *28*, 1166. [[CrossRef](#)] [[PubMed](#)]
48. Abdelmalek, F.; Ghezzer, M.R.; Belhajd, M.; Addou, A.; Brisset, J. Bleaching and degradation of textile dyes by nonthermal plasma process at atmospheric pressure. *Ind. Eng. Chem. Res.* **2006**, *45*, 23–29. [[CrossRef](#)]

49. Magureanu, M.; Mandache, N.B.; Parvulescu, V.I. Degradation of organic dyes in water by electrical discharges. *Plasma Chem. Plasma Process* **2007**, *27*, 589–598. [[CrossRef](#)]
50. Sousa, J.L.; Aguiar, A. Influence of aromatic additives on Bismarck Brown Y dye color removal treatment by Fenton processes. *Environ. Sci. Pollut. Res.* **2017**, *24*, 26734–26743. [[CrossRef](#)] [[PubMed](#)]

Disclaimer/Publisher’s Note: The statements, opinions and data contained in all publications are solely those of the individual author(s) and contributor(s) and not of MDPI and/or the editor(s). MDPI and/or the editor(s) disclaim responsibility for any injury to people or property resulting from any ideas, methods, instructions or products referred to in the content.